Hindawi
Geofluids
Volume 2022, Article ID 7808376, 11 pages
https://doi.org/10.1155/2022/7808376

Research Article

Study on the Influence of Excavation Unloading on Pile Depth in Sandy Soil

Huang Zhanjun,[1] Zou Yi,[2,3] Ding Haibin,[2,3] Liang Xinhuan,[1] Zhu Bitang,[2,3] and Jiang Yalong[2,3]

[1]*Nanchang Rail Transit Group Limited Corporation, Nanchang 330013, Jiangxi, China*
[2]*School of Civil Engineering and Architecture East China Jiaotong University, Nanchang 330013, China*
[3]*Engineering Research & Development Centre for Underground Technology of Jiangxi Province Nanchang 330013, China*

Correspondence should be addressed to Ding Haibin; hbding@ecjtu.edu.cn

Received 16 May 2022; Revised 7 July 2022; Accepted 13 July 2022; Published 28 July 2022

Academic Editor: Dongjiang Pan

With the development of urban construction, uplift pile has been widely used in underground structure bearing buoyancy. The pile is buried deep underground, and the foundation pit is excavated on the pile foundation, the stress redistribution of the soil after the foundation pit excavation will reduce the lateral stress of the pile at the bottom of the pit, resulting in the reduction of friction resistance, but this effect is limited to a certain depth at the bottom of the foundation pit. Referring to the unloading influence depth corresponding to the vertical unloading coefficient in the spring back calculation of foundation pit and introducing the unloading influence depth corresponding to the horizontal unloading coefficient, it is deduced that the relationship between the horizontal unloading coefficient and the vertical unloading coefficient is based on the friction angle. Based on the bearing capacity control and numerical simulation, it is determined that the corresponding depth when the horizontal unloading coefficient is 0.95 is the unloading influence depth. The depth to width ratio of excavation has a great influence on unloading influence depth, and the internal friction angle of soil has little influence on unloading influence depth, while the influences of pile diameter and pile-soil friction coefficient can be ignored. The formula of unloading influence depth is derived in this paper. Comparing the unloading influence depth of sand and soft soil, the unloading influence depth of sand is greater than that of soft soil.

1. Introduction

With the development of urban construction, uplift pile has been widely used in underground structure bearing buoyancy. The pile is buried deep underground, and the foundation pit is excavated on the pile foundation [1, 2]. The unloading of foundation pit excavation causes the stress redistribution of soil, which will reduce the bearing capacity of piles fabricated before the foundation pit excavation [3, 4]. This unloading effect is related to factors such as the scope of foundation pit excavation, soil body properties, and foundation pit exposure time [5]. The reduction effect of excavation unloading on the bearing capacity of pile is that the normal stress of pile side is reduced due to excavation unloading, and the reduction amount of the normal stress decreases with the increase of depth [6–8]. When reaching a critical depth, the reduction of the normal stress of pile side is not enough to affect its bearing capacity [9, 10]. For long piles, the influence of excavation unloading is complex and unnecessary to consider along the whole pile. The wrong estimation of the unloading influence range will overestimate the bearing capacity of the pile; thus, the research on the unloading influence depth is extremely necessary.

Soil mechanics [11] recommends that when the unloading ratio of normal soil and soft soil is 0.2 and 0.1, respectively, the corresponding depth is the depth limit, and the rebound of soil under the depth limit will be ignored. Pan [12] conducted the conventional consolidation rebound test on the shallow undisturbed silty clay sample in Wenzhou area and obtained that when the unloading ratio R is less

than 0.2, the rebound ratio of the preloaded soil sample is nearly 10^{-4}. Therefore, the unloading ratio $R = 0.2$ is regarded as the critical condition of rebound deformation. Liu et al. [13] set the residual stress coefficient at the limit depth considering the unloading effect as 0.95 and obtained the relevant empirical formula according to the engineering experience in Shanghai:

$$h_r = \frac{H}{0.0612H + 0.19}, \tag{1}$$

where H is the excavation depth of foundation pit, m; h_r is the influence depth of residual stress. Li [14] proposed that under the condition of large-area excavation and uniform unloading of foundation pit, the limit depth of soil rebound deformation at the bottom of the pit is 2H, and that in practical engineering is 1.5H. Zhou and Yang [15] studied the influence of excavation depth, excavation width, internal friction angle, and Poisson's ratio on the unloading influence calculation depth based on Mindlin solution, and modified it on the basis of Equation (1). Pan et al. [16] conducted direct shear test on undisturbed muddy clay soil samples taken from the construction site of Jinzhang highway in Pudong, Shanghai, and considered the influence of time factors. The relationship curve between unloading ratio and strength residual ratio at different times was obtained, and the empirical formula for the depth of the affected area was also obtained:

$$Z_{cr} = \frac{(1 - R_{cr})D}{R_{cr}} = 1.33D. \tag{2}$$

To sum up, the contents described in the calculation depth limit, rebound deformation critical condition, residual stress influence depth, and influence area depth are consistent. They are all trying to find the influence depth of excavation unloading; thus, they can be collectively called as unloading influence depth. The sum of the unloading ratio and residual stress coefficient corresponding to the unloading influence depth is 1. The former is the ratio of the reduction of vertical stress caused by unloading to the vertical stress of soil before unloading, and the latter is the ratio of the vertical stress after unloading to the stress before unloading. In this paper, the vertical (horizontal) unloading coefficient is unified to correspond to the unloading depth, and its calculation method is the same as the residual stress coefficient. The unloading influence shall be considered in the area at the bottom of the foundation pit and within the unloading influence depth. When the depth exceeds the unloading influence depth, the influence of unloading on the soil rebound or pile bearing capacity of this part of soil will not be considered. However, most of the above studies were focused on the influence depth of soil rebound strain control on unloading, and there is no research on the influence on pile bearing capacity. Besides, the above conclusions were regional, especially few of them studied and analyzed sand. The simulation software Plaxis3D is used to establish the foundation pit excavation model with single pile, and the HSS soil constitutive model is adopted by introducing the sand soil parameters in the stratum of Nanchang, to define the horizontal unloading influence coefficient corresponding to unloading influence depth. Besides, consider four factors of depth width ratio of the foundation pit, soil fiction angle, pile-soil friction coefficient, and pile diameter to deduce the calculation formula of unloading influence depth suitable for the sand soil in Nanchang district.

2. Calculation of Lateral Unloading Coefficient

When studying the unloading influence depth, the corresponding unloading coefficient should be found. In the rebound calculation of the foundation pit, the lateral unloading coefficient is the factor corresponding to the unloading influence depth. While for studying the friction pile, the bearing capacity of pile is related to the normal stress at the pile side. The deduction of the horizontal unloading coefficient is as follows:

Before the excavation of foundation pit, the calculation formula for the lateral effective stress at the depth z is as follows:

$$\sigma_z = \gamma z. \tag{3}$$

Based on the value of K/K_0 under different unloading conditions counted by Zhang et al. [17, 18] and combing the fact that the soil system in front of the pile has already been fully consolidated and dense before the excavation of the foundation pit, the calculation formula for the K value before unloading excavation is as follows:

$$K = 1 - \sin\varphi, \tag{4}$$

where φ is the effective internal friction angle.

The calculation formula for the horizontal effective stress before the excavation of foundation pit is as follows:

$$\sigma_h = (1 - \sin\varphi)\gamma z. \tag{5}$$

After the excavation of foundation pit, the calculation formula for the effective stress at the depth z is as follows:

$$\sigma_z' = \gamma z - p_t, \tag{6}$$

where P_t is the reduction of the lateral stress.

Considering the change of the consolidation degree after excavation, Gang et al. [10] and Mayne and Kulhawy [19] proposed that

$$K' = (1 - \sin\varphi)\mathrm{OCR}^{\sin\varphi}, \tag{7}$$

where OCR is the over consolidation ratio of soil, which equals to the ratio of the lateral effective stresses before and after excavation.

The calculation formula for the horizontal effective stress after the excavation of foundation pit is as follows:

$$\sigma_h' = (1 - \sin\varphi)\mathrm{OCR}^{\sin\varphi}(\gamma z - p_t). \tag{8}$$

The lateral unloading coefficient and over consolidation ratio are as follows:

$$\alpha_v = \frac{\gamma z - p_t}{\gamma z} = \mathrm{OCR}^{-1}. \tag{9}$$

By introducing the horizontal unloading coefficient and combined Equations (5), (8), and (9), the relationship between the horizontal and lateral unloading coefficients is deduced:

$$\alpha_h = \frac{\sigma_h'}{\sigma_h} = \mathrm{OCR}^{(\sin\varphi - 1)} = \alpha_V{}^{(1-\sin\varphi)}. \tag{10}$$

From Equation (10), it can be seen that the relationship between the horizontal and lateral unloading coefficients is affected by friction angle, and under the same lateral unloading coefficient, the larger the friction angle, the larger the horizontal unloading coefficient. Based on the lateral unloading coefficients of 0.8, 0.9, and 0.95 recommended in literature, the lateral unloading coefficients under the friction angel ranges from 30° to 35° are calculated [11–13], as listed in Table 1, and three average values of 0.9, 0.95, and 0.98 are adopted to study the horizontal unloading coefficient.

Table 1: α_H corresponding to α_V at the friction angle of 30° and 35°.

α_V	Friction angle/°	α_H	α_H
0.80	30.00	0.894	0.9
0.80	35.00	0.909	
0.90	30.00	0.949	0.95
0.90	35.00	0.956	
0.95	30.00	0.975	0.98
0.95	35.00	0.978	

3. Determination of Lateral Unloading Coefficient

In order to determine the lateral unloading coefficient, a 3D single pile model is established, and based on the effect of the bearing capacity of pile, the three horizontal unloading coefficients proposed in Table 1 are selected as the criteria for the unloading depth in following sections.

3.1. Engineering Introduction. The under constructed project of Aixihu Tunnel is mainly a highway and subway combined tunnel, with a total length of 2280 m. The strata being traversed are mainly medium weathered argillaceous siltstone. The typical cross section of the foundation pit is highway tunnel, with the width of 30 m and the depth of 11 m. The main retaining structure is supported by 800 mm/1000 mm thick underground continuous wall, and its buried depth is 24 m. There are three supports inside the foundation pit, the first is the concrete support with wall thickness of 16 mm, and the other two are the steel pipe support with diameter of 609 mm. The foundation pit in the subway tunnel is 11.4 m wide and 7.6 m deep, and bored piles are used as the retaining structure of the inner foundation pit.

Since the foundation pit project crosses the lake bottom and the main structure is in the deep water, the supporting piles at the lower part of the lattice column and the inner pit are used as uplift piles to resist the impact of buoyancy on the structure. Based on the geological survey report and relevant literature [12], the detailed soil parameters are listed in Table 2.

3.2. Finite Analysis. In this paper, the Plaxis 3D is used for numerical simulation, and a 3D single model is established, in which the solid elements are adopted for the soil body, engineering pile, and enclosure pile. Multisoil layers are included in practical engineering projects, and the mechanical parameters of each layer are not the same. In order draw a conclusion fitting for a wider range, the model estimation is simplified:

(1) The simulated soil body is single gravel sand layer, which is due to the fact that most of the soil body in the excavation range of the foundation pit of Aixihu Tunnel. The HSS constitutive model is applied for soil body, and Wanglin et al. [20] verified the accuracy of the parameters of this kind of soil body

(2) In order to obtain enough normal stress data at pile sides, a pile length exceeding the unloading influence range should be made sure. Therefore, a super long pile is constructed with $L = 80$ m, pile diameter $d = 0.8$ m, and the pile-soil friction angle is 0.7φ

(3) In order to obtain ideal results, the deformation of enclosure wall can be reduced by setting anchor rods and increasing the stiffness of the enclosure wall. Therefore, the influence of the deformation of foundation pit support on stress field of soil can be ignored

(4) At analysis, the excavation shape of the foundation pit is square, and the uplift pile is located in the center of the foundation pit. According to the theory of Randolph and Wroth [21], the influence radius of single pile is adopted as the side length of model, and the height is 100 m, with fixed boundary

As shown in Figure 1, based on the typical cross section of Aixihu Tunnel, the width of the foundation pit is $a = 30$ m in the model, and the excavation method of excavating the soil body in layers is adopted, with 1 m per layer. And bearing capacity analysis of pile is conducted at the excavation depth of $H = 5, 10, 20, 30$ m.

3.3. Comparative Analysis of Calculation Results. γ is defined as the friction increasing coefficient of the pile side, and the calculation formula is as follows:

$$\gamma = \frac{Q'}{Q}, \tag{11}$$

Table 2: Soil layer parameters.

Soil layer	μ	Γ /kN/m^3	γ_{sat}/kN/m^3	E_{50}^{ref}/MPa	E_{oed}^{ref}/MPa	E_{ur}^{ref}/MPa	G_0^{ref}/MPa	E/MPa	C /kPa	Φ /°
Plain fill	0.32	18.9	18.9	10	10	30	45	-	10	12
Silty clay	0.32	19.0	19	10.5	10.5	31.5	47.25	-	49.62	22.63
Fine sand	0.3	19.1	19.1	16	16	48	72	-	0	30
Silty clay	0.32	19.0	19.0	7	7	21	31.5	-	49.62	22.63
Coarse sand	0.3	19.6	19.6	28	28	84	126	-	0	34
Gravel sand	0.3	20.0	20	32	32	96	115.2	-	0	35
Round gravel	0.3	20.0	20	35	35	105	157.5	-	0	36
Strongly weathered sandstone	0.3	20.1	20.1	-	-	-	-	200	30	37
Moderately weathered sandstone	0.29	20.5	20.5	-	-	-	-	2890	200	37

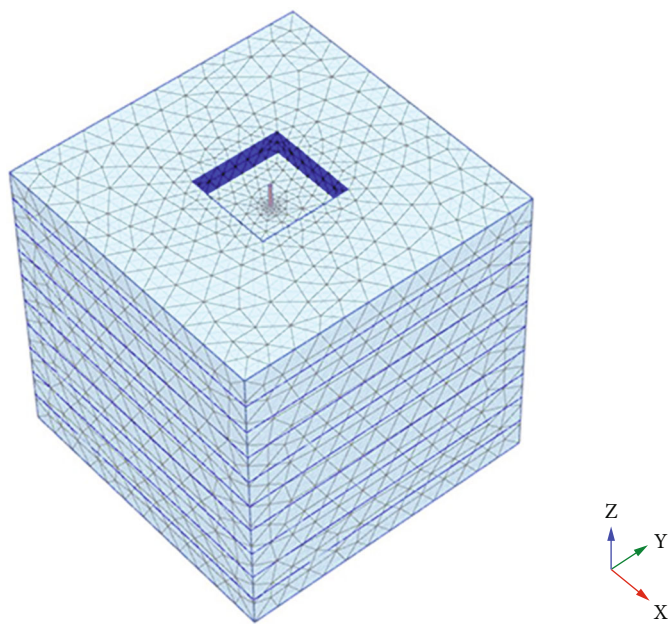

Figure 1: Numerical model of single pile.

where Q' is the friction of pile side considering the unloading influence depth and Q is the the friction of pile side not considering the unloading influence depth.

Figure 2 shows the changing curve of γ with the ratio of pile length to excavation depth (L/H). It can be seen that the lateral friction resistance of pile considering unloading effect depth is larger than that without unloading effect depth, because the former ignores the reduction of normal stress of pile under unloading effect depth. It also can be seen that, with the increase of L/H, γ increases first and then decreases. It can be explained in Figure 3 that OA is the normal stress curve of the pile before excavation, and $O'A'$ is the normal stress curve of the pile after excavation. The integral of the normal stress at each point over the length of pile is the total normal stress. Therefore, the total normal stress Q of pile after excavating is equal to the sum of the areas of ① and ② ($A1 + A2$), and the normal stress Q' of pile after excavating considering the influence depth is the sum of the areas of ①, ②, and ③ ($A1 + A2 + A3$). Then, the $\gamma = Q/Q' = (A1 + A2 + A3)/(A1 + A2) = 1 + 1/(A1/A3 + A2/A3)$. As pile length exceeds influence depth, $A1$ remains constant and $A2$ and $A3$ increase and then $A1/A3$ decreases, and $A2/A3$ increases. So the change in $A2/A3$ is less than the change in $A1/A3$, since $A2$ and $A3$ are small relative to $A1$, which leads to γ increases. When the increment of $A2/A3$ is equal to the reduction of $A1/A3$, the inflection point of γ curve appears, and with the increase of L/H, the γ curve gradually decreases until it is close to 1.

No matter how the excavation depth changes, the range of γ matches the horizontal unloading coefficient. When the horizontal unloading coefficient is 0.9, 0.95, and 0.98, the range of γ is 1-1.04, 1-1.02, and 1-1.008, respectively. Considering the unloading influence range, the calculation of bearing capacity of pile actually gives an overestimated result. When γ reaches 1.04, the condition is not safe. In practice, more errors by construction will always be introduced, and after the superposition of these two factors, the error may exceed 10%, which is unsafe in practical

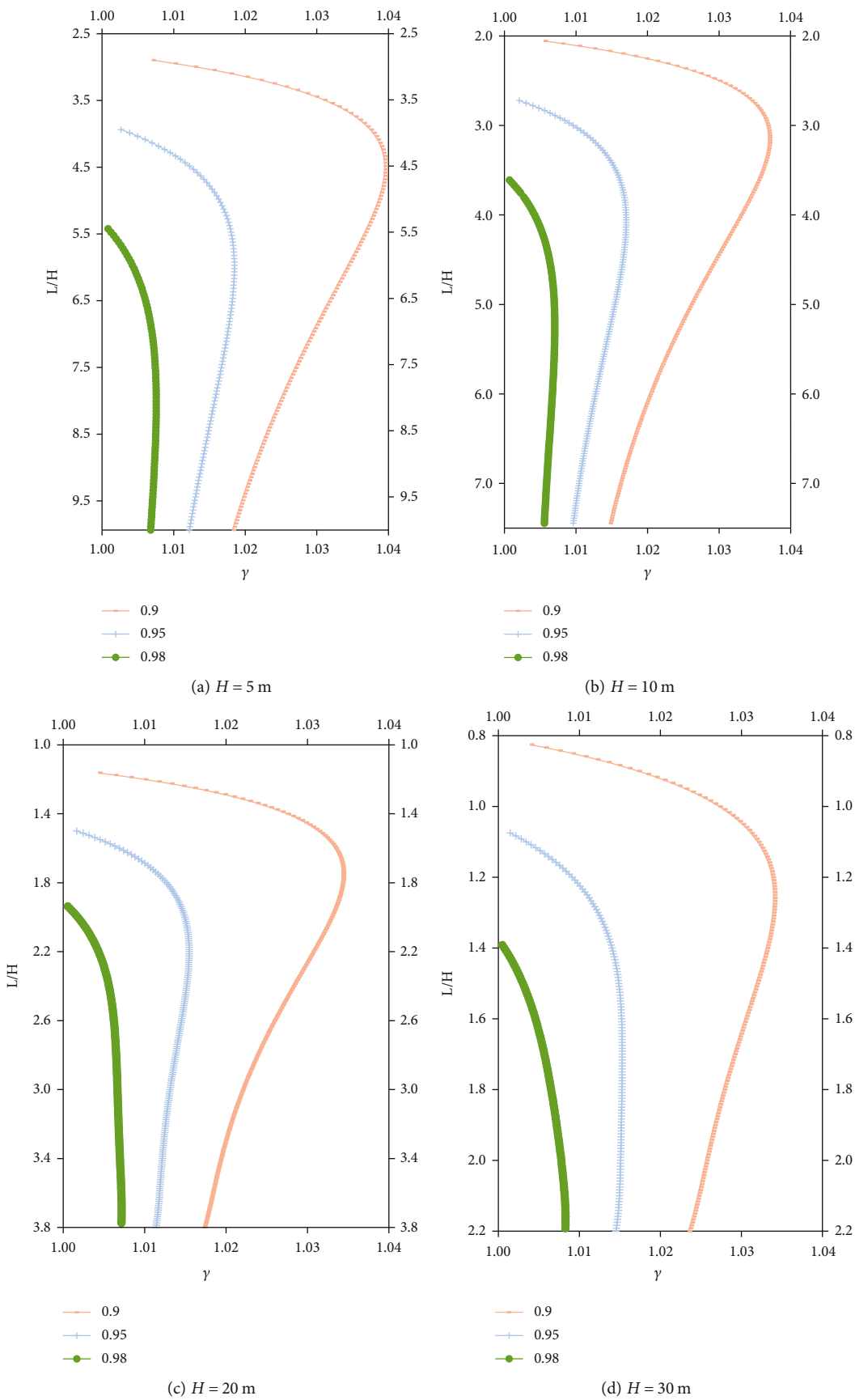

Figure 2: Change curve of increment coefficient of pile side friction resistance with L/H (ratio of pile length and excavation depth).

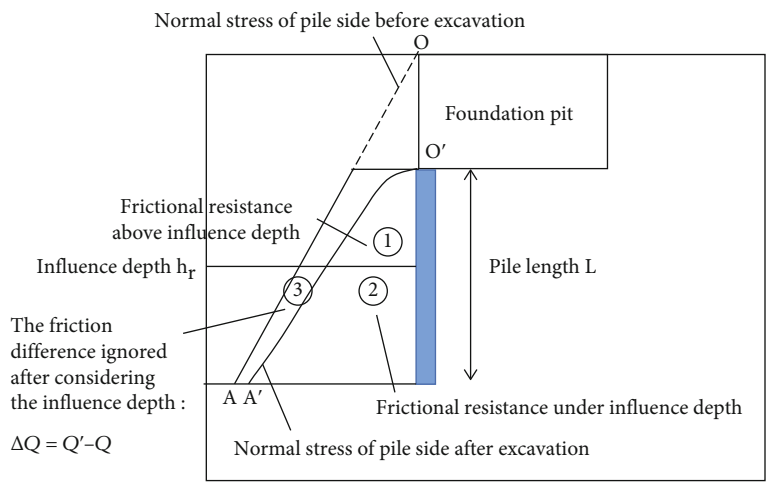

Figure 3: Illustration of the calculation area of pile side friction resistance.

engineering. In the γ range of 1-1.008, from the figure, it can be seen that under the excavation depth of $H = 5 - 20$ m, only when the pile length reaching 4-5 times of the original length can the bearing capacity satisfy the demand, meaning that the simplified calculation is too conservative. When γ is in the range of 1-1.02, the error is acceptable; therefore, 0.95 is selected as the criteria for determining the unloading influence depth.

4. Unloading Influence Depth

Based on the model in Section 3.2, 11 pile numerical models are established. According to the unloading influence depth under the horizontal unloading coefficient of 0.95, the influence of excavation depth width ratio, friction angle, pile diameter, and pile-soil friction coefficient on unloading influence depth is studied. Besides, the calculation formula suitable of unloading influence depth suitable for the sand soil in Nanchang is deduced, and the numerical simulation results of the soil body in Shanghai are compared and analyzed with those of Equation (1).

4.1. The Relationship between Parameter and Influence Depth

4.1.1. Influence of Excavation Depth Width Ratio on Unloading Influence Depth. In this section, the excavation is taken as $H = 5, 10, 20, 30$ m, five excavation side lengths of $a = b = 10, 20, 30, 40, 50$ m are defined, and the friction angle of soil body is $\varphi = 35^\circ$. The pile diameter $d = 0.8$ m, which is selected according to the design requirements, and the pile-soil friction coefficient $\delta = 0.7$, as shown in Table 3. Below, the relationship between the excavation depth ratio and the excavation depth width ratio is analyzed, and the formula of unloading influence depth as the function of excavation depth is deduced.

The scatter data in Figure 4 represent the unloading influence depth (in the figure, the excavation depth is normalized) obtained in the numerical simulation, under the 20 depth width ratios and in according with the horizontal unloading coefficient of 0.95. From this figure, it can be

Table 3: Parameters of simulation.

H/m	a/m	$\varphi/^\circ$	d/m	δ
5	10, 20, 30, 40, 50	35	0.8	0.7
10	10, 20, 30, 40, 50	35	0.8	0.7
20	10, 20, 30, 40, 50	35	0.8	0.7
30	10, 20, 30, 40, 50	35	0.8	0.7

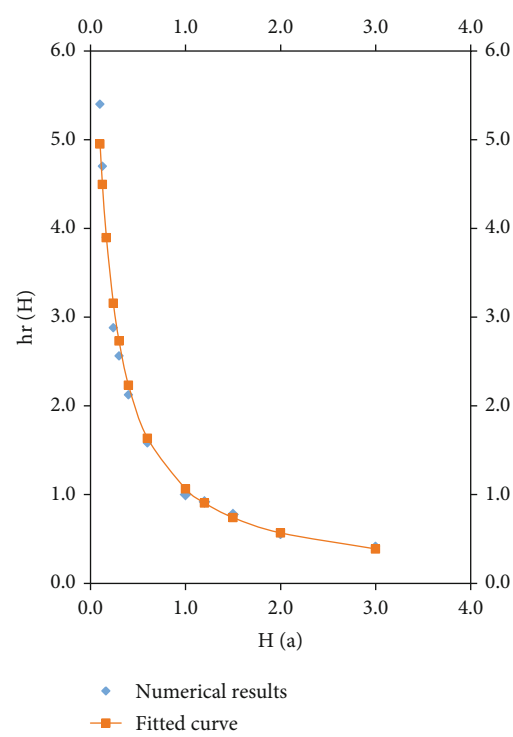

Figure 4: The relationship between ratio of unloading influence depth to excavation depth (hr/H) and the excavation depth width ratio (H/a).

clearly seen that there is a strong relationship between the ratio of unloading influence depth to excavation depth h_r/H and the excavation depth width ratio H/a; therefore, these data can be fitted, and the fitted formula is shown in Equation (12). And its correlation coefficient is 0.988, which indicates that the formula has good goodness of fit.

$$\frac{h_r}{H} = \frac{1}{0.82H/a + 0.120}. \tag{12}$$

From the fitted curves in Figure 4, it can be seen that the h_r/H is in a reverse relationship with H/a. Though simple conversion of the formula, it is found that with the increase of excavation depth, the h_r gradually converges to a constant, which is related to the side lengths of a and b (here the condition of a not equaling b is not discussed). Based on curves of numerical results and fitting formula, it can be seen that the fitted empirical formula has good fitting degree, and it can be used to calculate the unloading influence depth in a high accuracy.

4.1.2. Influence of Friction Angle on Unloading Influence Depth. In this section, the relationship between the excavation depth and friction angel of soil is analyzed. The excavation depth is set as $H = 5, 10,$ and 30 m, the excavation side length is set as $a = b = 30$ m, the friction angle of soil body $\varphi = 30^\circ, 33^\circ,$ and 35°, the pile diameter $d = 0.8$ m, and the pile-soil friction coefficient $\delta = 0.7$, as shown in Table 4.

From Figure 5, h_r/H tends to rise slightly with the increase of friction angle under three different excavation depths. This is due to the fact that the interaction between soil particles strengthens with the increasing friction angle, which enhances the unloading effect.

From the data in Figure 5, it can be found that the ratio of the hr/H under the friction angles of 30° and 33° to that under the friction angles of 35° is listed in Table 3, which integrates the ratio corresponding to the 3 excavation depths, and the median is taken as the representative value for analyzing the unloading influence depth.

It can be obtained from Table 5 that the difference of the last h_r/H is in consistence with that of the friction angle, thus the relation formula between the internal friction angle ratio and h_r/H ratio, as shown in Equation (13).

$$\frac{h_r(\varphi)}{h_r(35^\circ)} = 1 - \frac{0.04(35^\circ - \varphi)}{5}. \tag{13}$$

Substitute Equation (13) to Equation (12), and through modification, the modified calculation formula for the influence depth under unloading effect can be obtained:

$$h_r = H \cdot \frac{1 - 0.008(35^\circ - \varphi)}{0.82H/a + 0.12}. \tag{14}$$

4.1.3. Influence of Pile Diameter and Pile-Soil Friction Coefficient on Unloading Influence Depth. In this section, the relationship between the pile diameter and pile-soil friction coefficient is analyzed. The excavation depth is set as $H = 5, 10,$ and 30 m, the excavation side length is set as $a = b = 30$ m, and the friction angle of soil body $\varphi = 35^\circ$. When studying the pile diameter, the pile diameter is set as $d = 0.4, 0.6$ and 0.8 m, and the pile-soil friction coefficient $\delta = 0.7$. When studying the pile-soil friction coefficient, the pile diameter is set as $d = 0.8$ m, and the pile-soil friction coefficient $\delta = 0.7, 0.8, 0.9,$ and 1.0 [22]. The parameters are shown in Table 6.

Figure 6 shows the relationship between the unloading influence depth with the pile diameter and pile-soil friction

Table 4: Parameters of simulation.

H/m	a/m	$\varphi/^\circ$	d/m	δ
5	30	30,33,35	0.8	0.7
10	30	30,33,35	0.8	0.7
30	30	30,33,35	0.8	0.7

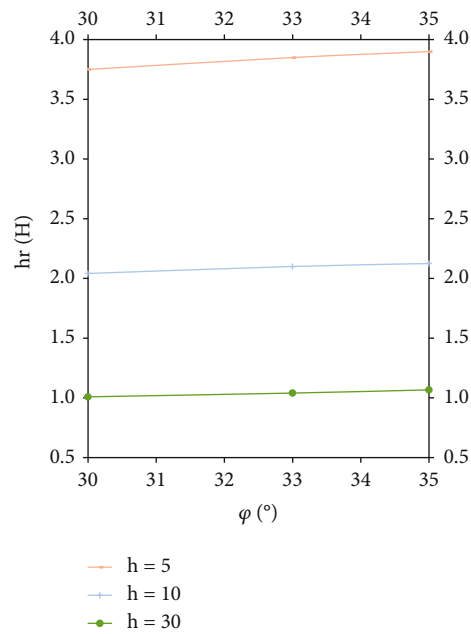

Figure 5: The relationship between unloading influence depth (h_r) and friction angle (φ).

Table 5: The ratio of $h_r/H(30^\circ, 33^\circ, 35^\circ)$ to $h_r/H(35^\circ)$.

φ (°)	$H = 5$ m	$H = 12$ m	$H = 30$ m	Value
30.00	0.96	0.96	0.94	0.95
33.00	0.99	0.99	0.97	0.98
35.00	1.00	1.00	1.00	1.00

Table 6: Parameters of simulation.

H/m	a/m	$\varphi/^\circ$	d/m	δ
5	30	35	0.4, 0.6, 0.8	0.7, 0.8, 0.9, 1.0
10	30	35	0.4, 0.6, 0.8	0.7, 0.8, 0.9, 1.0
30	30	35	0.4, 0.6, 0.8	0.7, 0.8, 0.9, 1.0

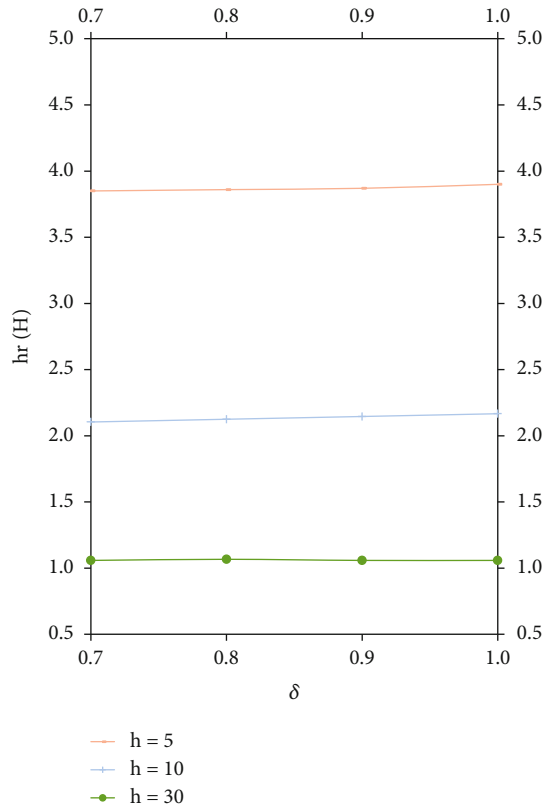

(a) Relationship between unloading influence depth (h_r) and pile-soil friction coefficient (δ)

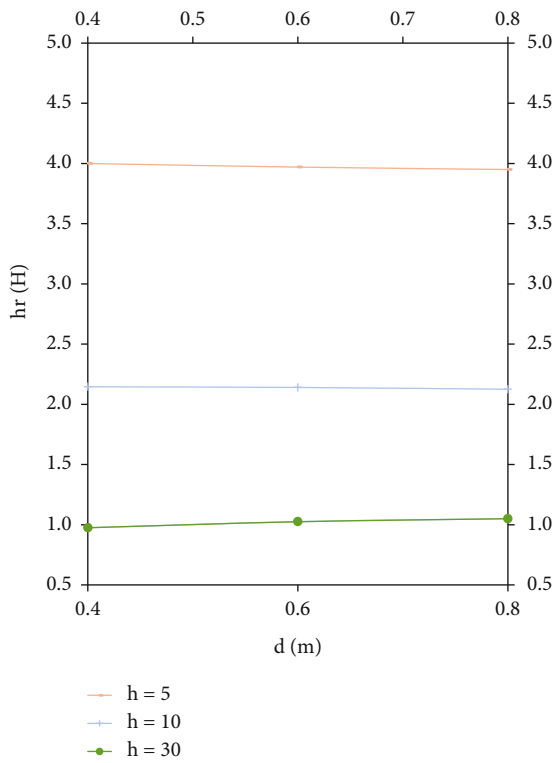

(b) Relationship between unloading influence depth (h_r) and pile diameter (d)

Figure 6: The relationship between unloading influence depth (h_r) with pile diameter (d) and pile-soil friction coefficient (δ).

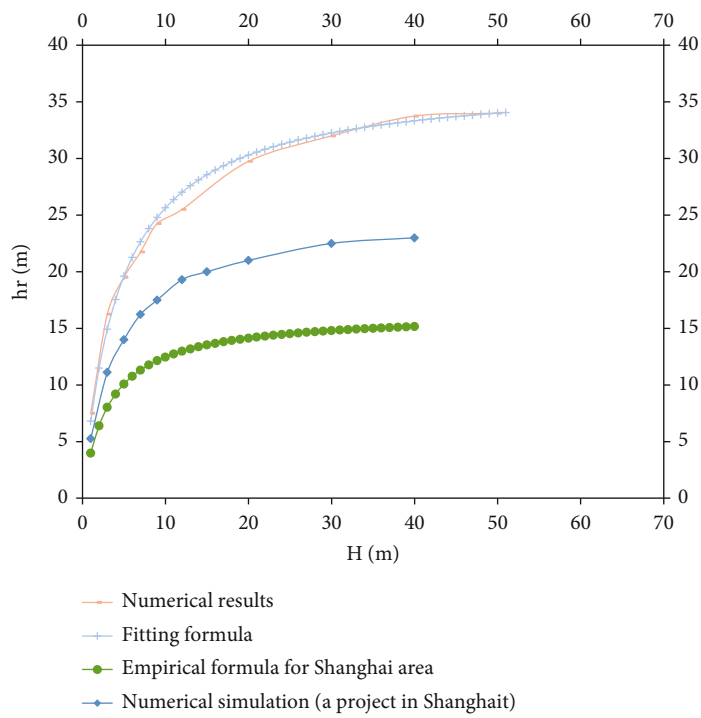

Figure 7: The comparison of unloading influence depth of sand soil and soft soil.

coefficient, and it can be seen the influence of pile diameter and pile-soil friction coefficient on the unloading influence depth is small and can be ignored.

From above analysis, a formula for calculating the excavation influencing depth in sand soil is obtained, by comprehensive consideration of geometric parameters of foundation pit excavation (excavation depth and excavation width), soil body parameters (friction angle), and pile parameters (pile diameter and pile-soil friction coefficient), as shown in Equation (14).

4.2. Comparison of the Unloading Influence Depth in Soil Sand and Soft Soil. In this section, the calculation formula deduced in the present work for sand soil and that for the soft soil in Shanghai are compared, and the former one comes from Equation (1) and numerical simulation.

As Equation (1) only considers the influence of excavation H on unloading depth, when it is compared with the formula deduced in the present work, the excavation width is set as $a = 30$ m and the friction angle of soil body is set as 35°, according to the typical excavation cross section of Aixihu Tunnel. Based on the whole set of HSS soil body parameters for the soft soil in Shanghai recommender in Reference [23], one model in the literature is established to analyze the influence depth of excavation unloading [24–37].

From Figure 7, it can be seen that

(1) In the empirical formula deduced in the present work from numerical simulation, Equation (1), and the numerical model based on practice engineering projects, the evolution law of the unloading influence depth with the excavation depth is the same, that is, the unloading influence depth increases with the increasing excavation depth, and when H reaches about 15 m, the unloading influence depth gradually converges and becomes stable

(2) The results of the soft soil in Shanghai deduced from Equation (1) and numerical simulation are similar but there is certain difference, which is mainly due to the fact that Equation (1) is a semiempirical model summarized from real measured data, while the numerical simulation is only based on the engineering project in Shanghai, and the unloading exposure time cannot be considered. Even though, it can still be proved that the deduction for unloading influence depth from numerical simulation method is reliable

(3) The unloading influence depth of the sand soil in Nanchang (mainly the gravel sand in Aixihu Lake) is larger than the soft soil in Shanghai. Compared with sand soil, the mechanical properties of soft clay are more similar to plastic materials. When the soil body is loaded or unloaded, the stress and strain in the soil body similar to elastic materials are able to spread widely, while the soil body similar to plastic materials is just the opposite; thus, the unloading influence depth of sand soil is larger than that of soft soil

5. Conclusions

In this paper, the influence depth of horizontal unloading and vertical unloading is studied, the relationship between horizontal unloading coefficient and vertical unloading coefficient is found, and the equation expressing the relationship

between them is deduced. Based on the bearing capacity controlling and numerical simulation, the excavation depth corresponding to the lateral unloading coefficient of 0.95 is taken as the unloading influence depth. The following conclusions can be obtained:

(1) The influence of excavation depth width ratio on the calculated depth is significant, and the influence of the internal friction angle of soil body is small, but the influence of pile diameter and pile-soil friction coefficient can be ignored. And the calculation formula considering the depth to width ratio of excavation and internal friction angle of soil is derived

(2) The unloading influence depth of sand soil is larger than that of soft soil. This is because compared with sand soil, the mechanical properties of soft clay are more similar to plastic materials. When the soil body is loaded or unloaded, the stress and strain in the soil body similar to elastic materials are able to spread widely, while the soil body similar to plastic materials is just the opposite

Data Availability

Some data, models, or code generated or used during the study are available from the corresponding author upon request.

Conflicts of Interest

The authors declare that there are no conflicts of interest regarding the publication of this paper.

Acknowledgments

This work was supported by the Nanchang Rail Transit Group Scientific Research Project (2019HGKYB002), the National Science Fund of China (Grant Nos. 51878276 and 12172130), and the Natural Science Foundation of Jiangxi Province (Grant Nos. 20202ACB211002, 20212BAB204012, 20212BBE53016, and 20192ACB20001).

References

[1] L. Guo-bin, H. Yuan-Xiong, and H. Xie-Yuan, "A practical method for calculating a heave of excavated foundation," *China civil Engineering Journal*, vol. 33, no. 4, p. 7, 2000.

[2] R. Zhang, J. Zheng, H. Pu, and L. Zhang, "Analysis of excavation-induced responses of loaded pile foundations considering unloading effect," *Tunnelling and Underground Space Technology*, vol. 26, no. 2, pp. 320–335, 2011.

[3] G. Zheng, Y. Diao, and C. Ng, "Finite element analysis on mechanism of effect of extra-deep excavation on vertical load transfer and settlement of a single pile," *Chinese Journal of Geotechnical Engineering*, vol. 31, no. 6, pp. 837–845, 2009.

[4] G. Anthony, "Pile behaviour from excavation-induced soil movements," in *Proc Pan-American Conference on Soil Mechanics & Geotechnical Engineering*, 2013.

[5] D. E. Ong, C. E. Leung, and Y. K. Chow, "Pile behavior due to excavation-induced soil movement in clay. I: stable wall," *Journal of Geotechnical & Geoenvironmental Engineering*, vol. 132, no. 1, pp. 36–44, 2006.

[6] C. Jin-jian, W. Qiong, W. Jian-hua, and X. H. Wang, "Model tests on bearing capacity of single pile influenced by excavation," *Chinese Journal of Geotechnical Engineering*, vol. 32, no. S2, pp. 85–88, 2010.

[7] Y. Iwasaki, H. Watanabe, M. Fukuda, A. Hirata, and Y. Hori, "Construction control for underpinning piles and their behaviour during excavation," *Geotechnique*, vol. 44, no. 4, pp. 681–689, 1994.

[8] *International Journal of Rock Mechanics & Mining Sciences & Geomechanics Abstracts*, vol. 32, no. 4, p. A193, 1995.

[9] G. Zheng, Y. Diao, and C. W. W. Ng, "Parametric analysis of the effects of stress relief on the performance and capacity of piles in nondilative soils," *Canadian Geotechnical Journal*, vol. 48, no. 9, pp. 1354–1363, 2011.

[10] Z. Gang, S. Y. Peng, C. Ng, and Y. Diao, "Excavation effects on pile behaviour and capacity," *Canadian Geotechnical Journal*, vol. 49, no. 12, pp. 1347–1356, 2012.

[11] L. I. Guang-Xin, Z. H. A. N. G. Bing-Yin, and Y. U. Yu-zhen, *The Soil Mechanics*, Tsinghua University Press, 2nd edition, 2013.

[12] P. A. N. You-Lin and H. U. Zhong-Xiong, "Experimental study on the resilience of pit under unloading," *Chinese Journal of Geotechnical Engineering*, vol. 24, no. 1, pp. 101–104, 2002.

[13] L. I. U. Guo-Bin and H. O. U. Xue-Yuan, "Analysis of residual stress in heave deformation of soft soil foundation pit," *Underground Engineering and Tunnels*, vol. 2, p. 6, 1996.

[14] L. I. Chao, "Study on the application of pile foundation underpinning in the basement-addition of existing buildings," College of Civil Engineering, Southeast University, Nanjing, 2008.

[15] Z. Pin-Gui and Y. Xue-Lin, "An equivalent method for calculating side friction of pile considering excavation-induced unloading effect," *Rock and Soil Mechanics*, vol. 37, no. 10, p. 8, 2016.

[16] P. Lin-You, C. Yu-Mei, and H. Zhong-Xiong, "Experimental study on the shear strength of clay under the unloading state," *Rock and Soil Mechanics*, vol. 22, no. 4, 2016.

[17] J. Jaky, "Pressure in soils," *Proc Icsmfe*, pp. 103–107, 1948.

[18] Z. Qian-Qin, L. Shu-Cai, L.-p. Li, and Y. J. Chen, "Simplified method for settlement prediction of pile groups considering skin friction softing and end resistance hardening," *Chinese Journal of Rock Mechanics and Engineering*, vol. 32, no. 3, pp. 615–624, 2013.

[19] P. W. Mayne and F. H. Kulhawy, "K-OCR relationships in soil: J Geotech Engng Div ASCE, V108, NGT6, June 1982, P851-872," *International Journal of Rock Mechanics & Mining Sciences & Geomechanics Abstracts*, vol. 20, no. 1, pp. A2–A2, 1983.

[20] W. Lin, Z. Sheng-Yu, Z. Yue-Ming, J. Ya-Long, S. Ce-Hui, and Z. Bi-Tang, "Study on deformation of deep excavation for metro stations in river terraces in Nanchang," *Journal of East China Jiaotong University*, vol. 38, no. 3, p. 10, 2021.

[21] M. F. Randolph and C. P. Wroth, "An analysis of the vertical deformation of pile groups," *Géotechnique*, vol. 29, no. 4, pp. 423–439, 1979.

[22] J. G. Potyondy, "Skin friction between various soils and construction materials," *Géotechnique*, vol. 11, no. 4, pp. 339–353, 1961.

[23] G. Xiao-Qiang, W. Rui-Tuo, L. Fa-Yun, and G. Gao, "On HSS model parameters for Shanghai soils with engineering

verification," *Rock and Soil Mechanics*, vol. 42, no. 3, pp. 833–845, 2021.

[24] W. Zhong, J. Ouyang, D. Yang, X. Wang, Z. Guo, and K. Hu, "Effect of the in situ leaching solution of ion-absorbed rare earth on the mechanical behavior of basement rock," *Journal of Rock Mechanics and Geotechnical Engineering*, 2021.

[25] W. Hao, G. Zhao, and S. Ma, "Failure behavior of horseshoe-shaped tunnel in hard rock under high stress: phenomenon and mechanisms," *Transactions of Nonferrous Metals Society of China*, vol. 32, no. 2, pp. 639–656, 2022.

[26] M. He, Z. Zzhiqiang, Z. Jiwei, and L. Ning, "Correlation between the constant mi of Hoek-Brown criterion and porosity of intact rock," *Rock Mechanics and Rock Engineering*, vol. 55, no. 2, pp. 923–936, 2022.

[27] X. L. Li, Z. Y. Cao, and Y. L. Xu, "Characteristics and trends of coal mine safety development," *Part A: Recovery, Utilization, and Environmental Effects*, pp. 1–19, 2020.

[28] S. M. Liu, X. L. Li, D. K. Wang, and D. Zhang, "Investigations on the mechanism of the microstructural evolution of different coal ranks under liquid nitrogen cold soaking," *Energy Sources, Part A: Recovery, Utilization, and Environmental Effects.*, pp. 1–17, 2020.

[29] X. L. Li, S. J. Chen, Q. M. Zhang, X. Gao, and F. Feng, "Research on theory, simulation and measurement of stress behavior under regenerated roof condition," *Geomechanics and Engineering.*, vol. 26, no. 1, pp. 49–61, 2021.

[30] X. L. Li, S. J. Chen, S. M. Liu, and Z. H. Li, "AE waveform characteristics of rock mass under uniaxial loading based on Hilbert-Huang transform," *Journal of Central South University.*, vol. 28, no. 6, pp. 1843–1856, 2021.

[31] X. L. Li, S. J. Chen, S. Wang, M. Zhao, and H. Liu, "Study on in situ stress distribution law of the deep mine taking Linyi Mining Area as an example," *Advances in Materials Science and Engineering*, vol. 2021, no. 4, Article ID 5594181, 11 pages, 2021.

[32] H. Y. Liu, B. Y. Zhang, X. L. Li et al., "Research on roof damage mechanism and control technology of gob-side entry retaining under close distance gob," *Engineering Failure Analysis*, vol. 138, no. 5, article 106331, 2022.

[33] B. Liu, S. Yu, and Z. Chu, "Time-dependent safety of lining structures of circular tunnels in weak rock strata," *International Journal of Mining Science and Technology*, 2022.

[34] A. I. Lawal, S. Kwon, O. S. Hammed, and M. A. Idris, "Blast-induced ground vibration prediction in granite quarries: an application of gene expression programming, ANFIS, and sine cosine algorithm optimized ANN," *International Journal of Mining Science and Technology*, vol. 31, no. 2, pp. 265–277, 2021.

[35] Y. Xin, P. Gou, and F. Ge, "Analysis of stability of support and surrounding rock in mining top coal of inclined coal seam," *International Journal of Mining Science and Technology*, vol. 24, no. 1, pp. 63–68, 2014.

[36] L. Dong, Q. Tao, H. Qingchun et al., "Acoustic emission source location method and experimental verification for structures containing unknown empty areas," *International Journal of Mining Science and Technology*, vol. 32, no. 3, pp. 487–497, 2022.

[37] H. Farhadian, "A new empirical chart for rockburst analysis in tunnelling: tunnel rockburst classification (TRC)," *International Journal of Mining Science and Technology*, vol. 31, no. 4, pp. 603–610, 2021.